The Absence of ALTERNATIVE OXIDASE1a in Arabidopsis Results in Acute Sensitivity to Combined Light and Drought Stress[W][OA]

Estelle Giraud, Lois H.M. Ho, Rachel Clifton, Adam Carroll, Gonzalo Estavillo, Yew-Foon Tan, Katharine A. Howell, Aneta Ivanova, Barry J. Pogson, A. Harvey Millar, and James Whelan*

Australian Research Council Centre of Excellence in Plant Energy Biology, University of Western Australia,

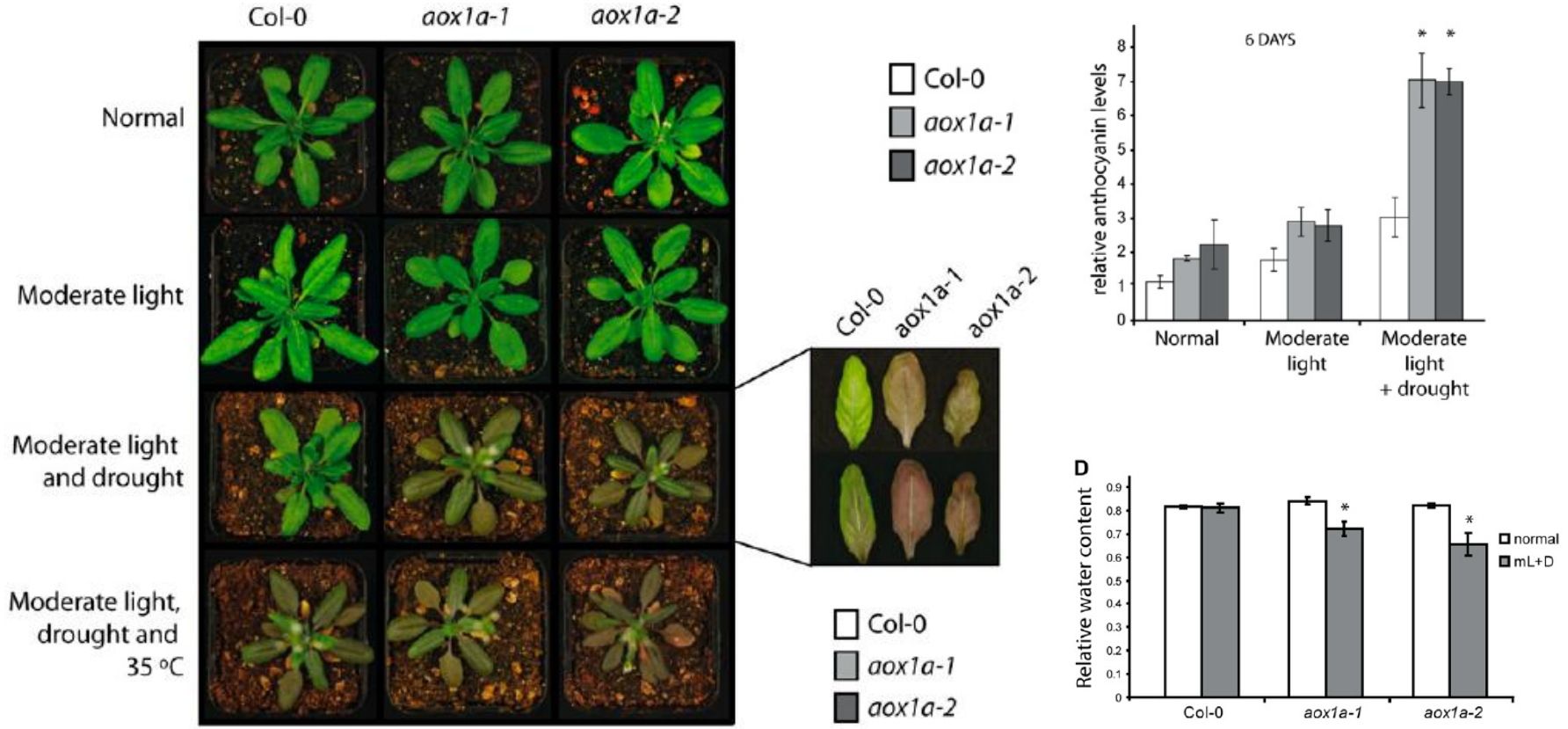

Plant Physiology, June 2008, Vol. 147, pp. 595–610,

O_2^- detection by nitroblue tetrazolium

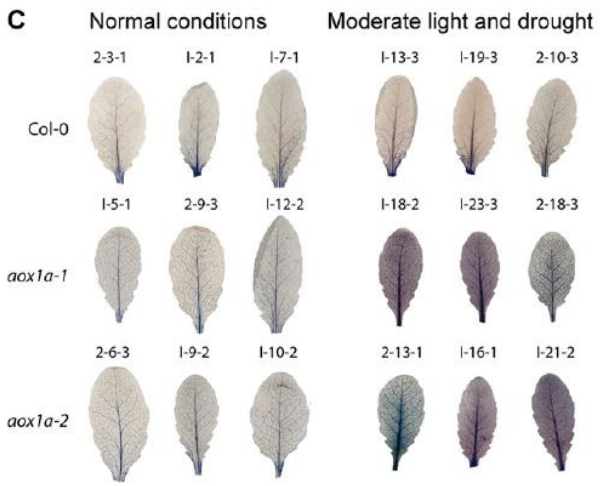

differences could be broadly classed as **decreases in amino acids and organic acids** and **increases in sugars**. This kind of metabolic pattern is consistent with the notion that loss of AOX1a could form a **constriction of primary metabolism** in *aox1a* plants by **decreasing the capacity of the tricarboxylic acid (TCA) cycle to operate uncoupled from oxidative phosphorylation**

aox1a Plants Display Altered Metabolite Profiles GC-MS

Metabolite Class	Metabolite Name	Fold Difference: *aox1a*/*col-0*	
		Unstressed	ML+D
Organic acids	cis-Aconitate	0.72	0.65
	cis-Sinapinate[a]	1.00	0.41
	Glycerate	1.18	0.36
	trans-Sinapinate[a]	1.01	0.37
	Unknown organic acid [4-hydroxybenzoic acid (2TMS), 88]	1.13	0.64
Amino acids	Ala	0.88	0.20
	Homo-Ser	0.89	0.30
	Leu	0.75	0.44
	Pyro-Glu	0.64	0.27
	Unknown amino acid [*N*-acetyl-Gly (1TMS), 71]	1.04	0.35
Sugars and sugar derivatives	Unknown sugar [arabinofuranose (4TMS), 70]	1.02	2.1
	Unknown sugar [arabinofuranose (4TMS), 74]	0.94	1.9
	Unknown sugar [D-glycero-D-gulo-heptose methoxime (6TMS), 79]	1.18	1.4
	Unknown sugar [Glc (5TMS), 82]	1.34	2.0
	Unknown sugar [melibiose (8TMS), 76]	1.07	4.7
	Unknown sugar [melibiose (8TMS), 83]	1.21	9.3
	Unknown sugar [sedoheptulose methoxime (6TMS), 85]	1.17	1.5
Sugar acids	Glucuronate	0.90	1.8
	Unknown sugar acid [D-glucuronic acid (5TMS), 79]	0.81	0.26
Polyols	Galactitol	1.13	1.6
Antioxidants	γ-Tocopherol	2.75	5.9
Inorganic acids	Phosphate	0.68	0.21

Table II. *Metabolite level differences between aox1a lines and Col-0 under normal growth and environmental stress conditions*

Metabolite levels were compared between *aox1a* and Col-0 lines under normal watering and light conditions and after 3 d of moderate light and drought using GC-MS-based metabolite profiling (see "Materials and Methods"). The mean fold difference (between *aox1a* and Col-0) in GC-MS signal levels (across the two independent *aox1a* lines) are shown for metabolites that responded similarly in both *aox1a* lines. The fold differences under normal growth conditions are shown in the "Unstressed" column, while the fold differences under the stress conditions are given in the "ML+D" (moderate light and drought) column. Metabolite signals that were significantly higher ($P < 0.05$, $n = 5$) in both *aox1a* lines are highlighted in blue, while signals that were significantly lower ($P < 0.05$, $n = 5$) are highlighted in red. Signals that were not significantly different from Col-0 in either *aox1a* line are shown in black. Color intensities are related to metabolite response intensities, with more strongly responsive signals highlighted in brighter tones. Compounds shown in square brackets are unknown metabolites with mass spectral homology to the indicated compound, with the number after the compound name being the "simple" match score reported by AMDIS when searched against the NIST02 MS library.

Microarray analysis (MapMan software). Overview of changes in transcript abundance associated with primary metabolism significantly changed **between aox1a and Col-0 under moderate light and drought treatment conditions (decreases** in transcripts of genes encoding proteins involved in **photosynthesis**, **photorespiration**, and **cell wall** metabolism and **increases** in transcripts for genes encoding components of **Suc and starch metabolism** and **flavonoid** production were observed)

* Under **normal conditions:** increases in transcript abundance for genes encoding proteins involved in cell wall modification and synthesis and lipid synthesis, photorespiration and antioxidant defense.

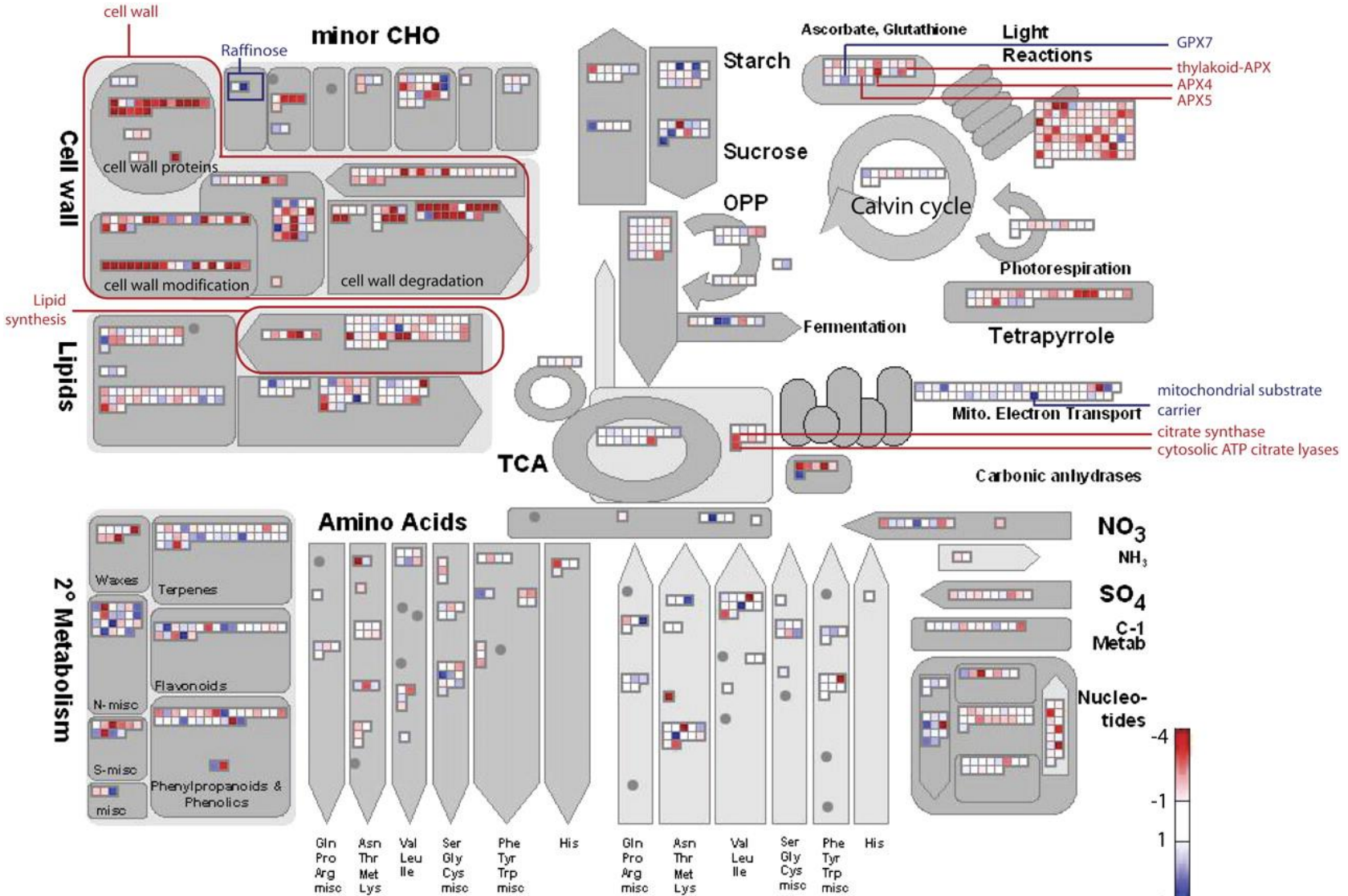

Large differences in the transcriptome between aox1a and Col-0 are supported by PCA: Large difference between aox1a in normal conditions versus treatment. Differences between aox1a and Col-0 under normal conditions are also evident, and while there are smaller difference between Col-0 normal and treated samples.

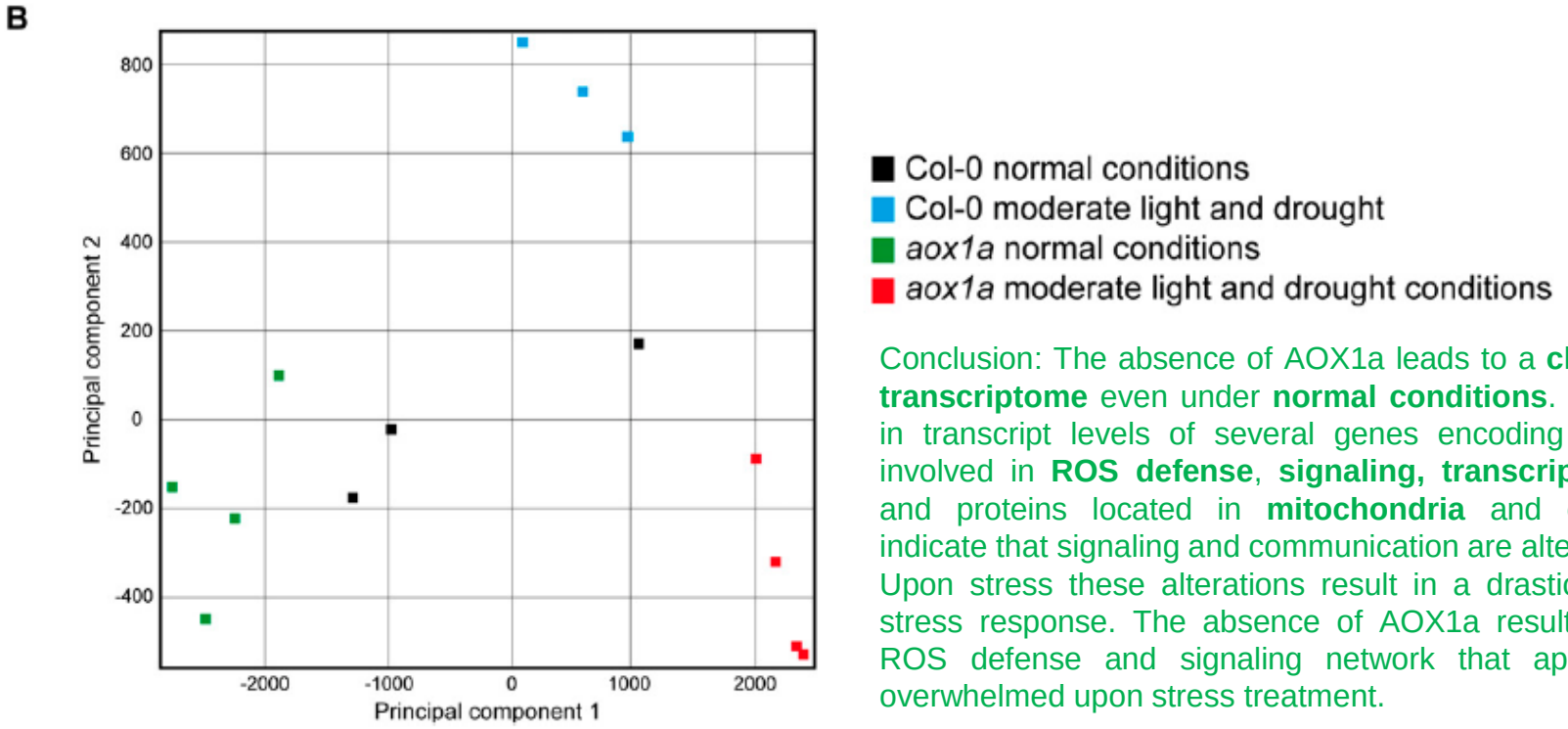

Conclusion: The absence of AOX1a leads to a **change in the transcriptome** even under **normal conditions**. The changes in transcript levels of several genes encoding components involved in **ROS defense**, **signaling, transcription** factors, and proteins located in **mitochondria** and **chloroplasts** indicate that signaling and communication are altered.
Upon stress these alterations result in a drastically different stress response. The absence of AOX1a results in a basal ROS defense and signaling network that appears to be overwhelmed upon stress treatment.

Figure 4. Whole transcriptome analysis of the response of Col-0 and *aox1a* lines to moderate light and drought treatment. A, Changes in transcript abundance between Col-0 and *aox1a* under moderate light and drought treatment. FC (all) refers to the number of genes called present in the array, FC > 1.5 refers to the number of genes with an expression fold change of 50% or more, and FC > 3.0 refers to the number of genes with an expression fold change greater than 200%. *P* (all) represents the number of genes matching the FC criteria for which a *P* value was calculated, while *P* (corrected) represents the number of genes matching the FC criteria with a *P* value of 0.05 or less when corrected for FDR according to a method based on Benjamini and Hochberg (1995), a q value computation. B, PCA of the above changes to obtain an overall view of the differences between genotypes and treatments.

Thermogenesis is restricted to relatively few plant species.

In non-thermogenic plants, synthesis of AOX is **up-regulated** at the transcriptional level by **several biotic and abiotic stresses**, including cold stress. However, the cold induction is clearly not to heat the tissue. During cold stress, **reactive oxygen species (ROS)** are formed, and other stress treatments that lead to elevated ROS also induce AOX.

ROS (e.g., superoxide and hydrogen peroxide) are formed as **by-products of electron transport under aerobic conditions**. ROS can cause damage to proteins, lipids, and DNA and the cell must therefore limit their formation

AOX helps prevent overreduction of the ETC and thus lowers ROS production. **Overexpression of AOX** in cultured cells lowered the steady state level of ROS, whereas **suppression of AOX** increased it. Similar results have been observed in **intact plants**. These results point to the mitochondrion as an important site of ROS generation and ROS signaling in plant cells

Respiração

Eléctrodo de oxigénio
"Clark-type"

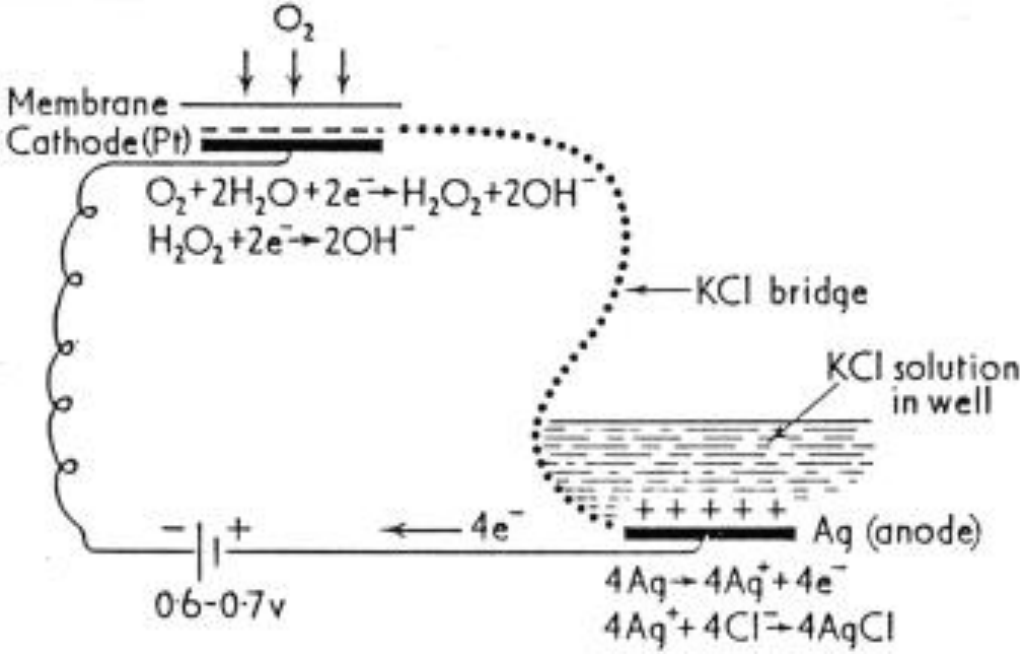

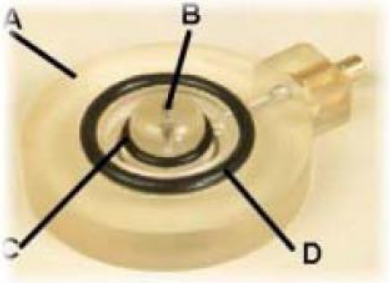

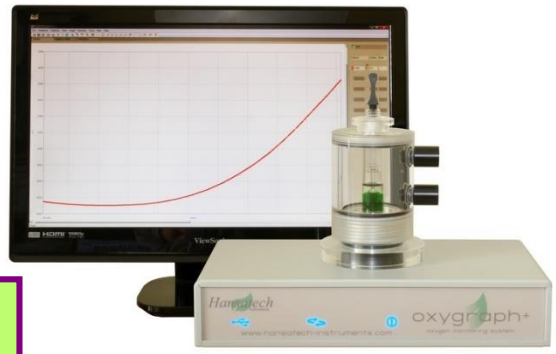

Eléctrodo ligada a uma unidade de controle que estabelece um potencial entre a platina e a prata (700 mV). No cátodo de platina o O_2 é reduzido e a corrente passa através do circuito (fuma fina camada de KCl serve de electrólito). A prata (ânodo) é oxidada depositando-se cloreto de prata

A respiração faz diminuir a concentração de O_2 na câmara e no cátodo e a voltagem diminui proporcionalmente.

Temperatura, Calibração (100%, 0%)

Respiração

Arabidopsis thaliana WT e AS-*aox1a*

Plant Physiology, December 2005, Vol. 139, pp. 1806–1820,

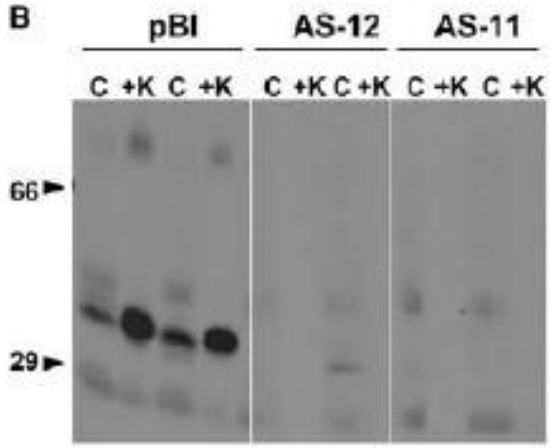

Figure 1. Immunoblots of AOX in whole-leaf tissue extracts

5 genes em Arabidopsis , AOX1a é a isoforma mais abundante nas folhas

-aox1a
-Aox1b
-Aox1c
-Aox1d
-Aox2

Respiração

Arabidopsis thaliana WT e AS-*aox1a*

KCN SHAM

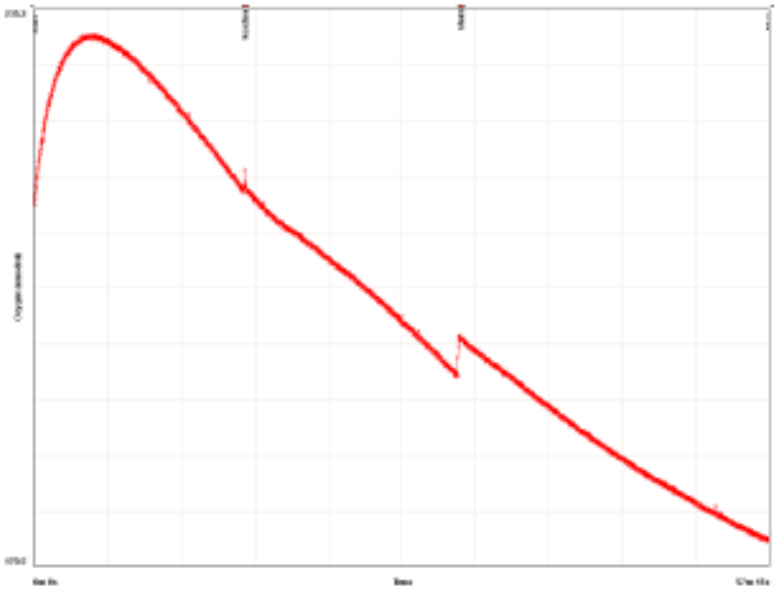

Declives ($nmolO_2\ min^{-1}$)

WT :

Inicial : -1,9

KCN: -1,14

SHAM: -0,8

KCN SHAM

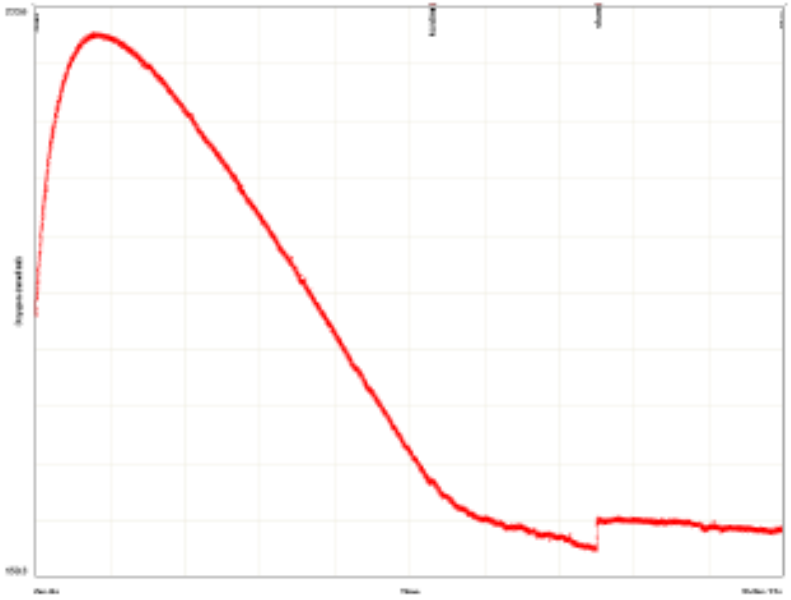

Declives :

AS-aox1a:

Inicial : -2,2

KCN: -0,37

SHAM: -0,12

Isotope fractionation: AOX activity *in vivo*

Mass spectrometry-liquid or gas phase measurements

ABSTRACT: The reduction chemistry of molecular oxygen underpins the energy metabolism of multicellular organisms, liberating free energy needed to catalyze a plethora of enzymatic reactions. Measuring the isotope signatures of ^{16}O and ^{18}O during O_2 reduction can provide insights into both kinetic and equilibrium isotope effects. However, current methods to measure O_2 isotope signatures are time-consuming and disruptive. This paper describes the application of membrane inlet mass spectrometry to determine the oxygen isotope discrimination of a range of O_2-consuming reactions, providing a rapid and convenient method for determining these values. A survey of oxygenase and oxidase reactions provides new insights into previously uncharacterized amino acid oxidase enzymes. Liquid and gas phase measurements show the ease of assays using this approach for purified enzymes, biological extracts and intact tissues.

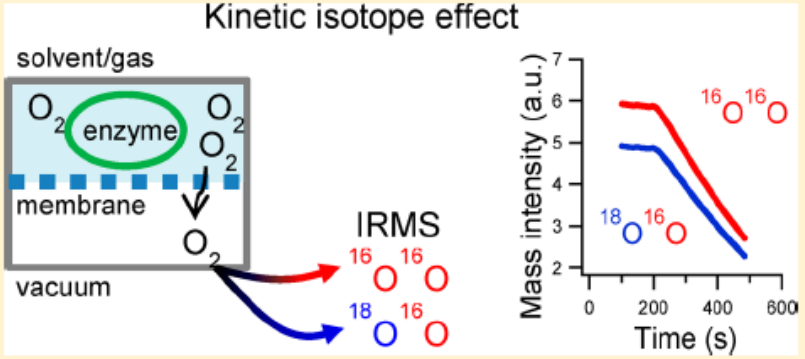

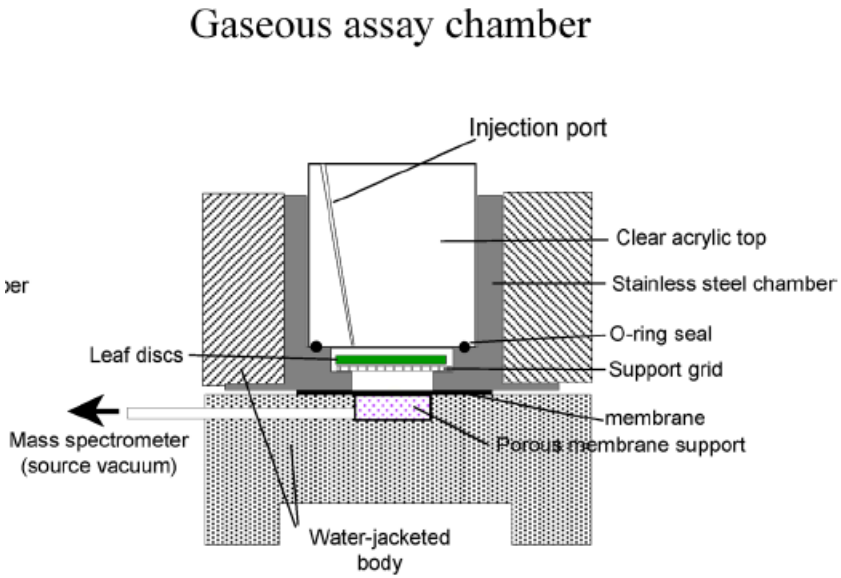

Plant respiration: the two **terminal oxidase** enzyme complexes, cytochrome c oxidase (CcO) and the di-iron alternative oxidase (AOX), **compete** for electrons in the mitochondrial electron transport chain where each are coupled to **different efficiencies of ATP synthesis** through the plant respiratory process. The fact that **they show different heavy ^{18}O isotope fractionation** has enabled differential fluxes to be determined **in vivo**

dx.doi.org/10.1021/ac501086n | Anal. Chem. 2014, 86, 5171−5178

In the heat of the night - alternative pathway respiration drives thermogenesis in *Philodendron bipinnatifidum*

Mass spectrometry

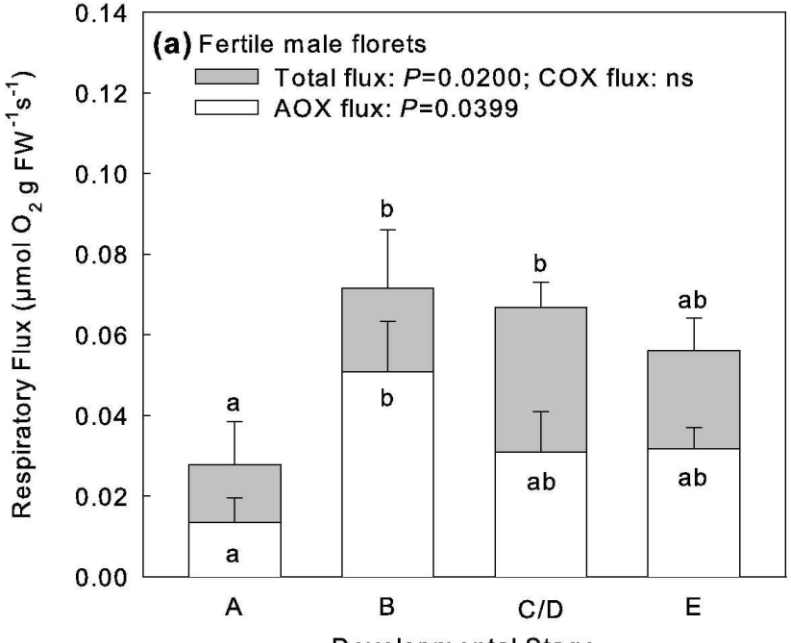

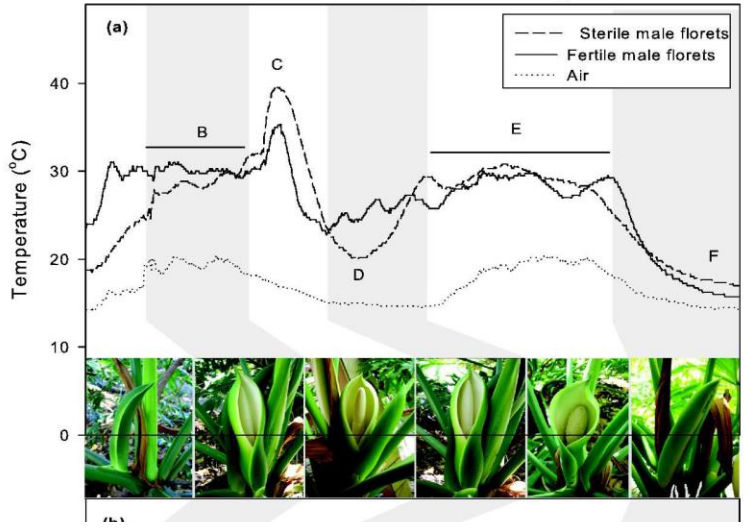

Protein detection by antibodies

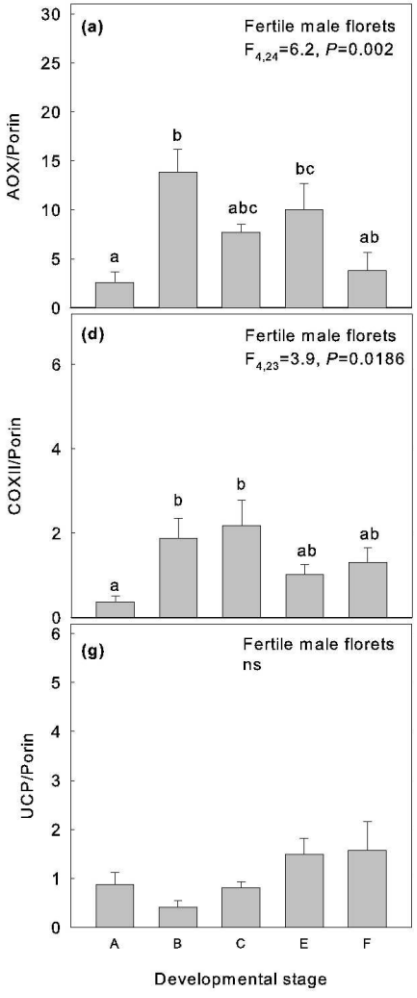

Inflorescences **heat up to 42ºC**. AOX contributed more than **90%** of respiratory flux during peak heating. **AOX protein increased 5-fold** with the onset of thermogenesis, whereas **UCP remained low** throughout development. These data indicate that AOX is primarily responsible for heating.

No direct correlations between AOX content and respiratory flux via the AOX in fertile-male florets, indicating that regulation of AOX activity is **post translational.**

Total respiratory flux (grey +white) and fluxes through the **AOX** (white) and **COX** (grey) pathways by developmental stage in **fertile male florets.**

DOI: 10.1111/j.1469-8137.2010.03547.x

ALTERNATIVE OXIDASE is regulated at the gene expression and protein activity levels

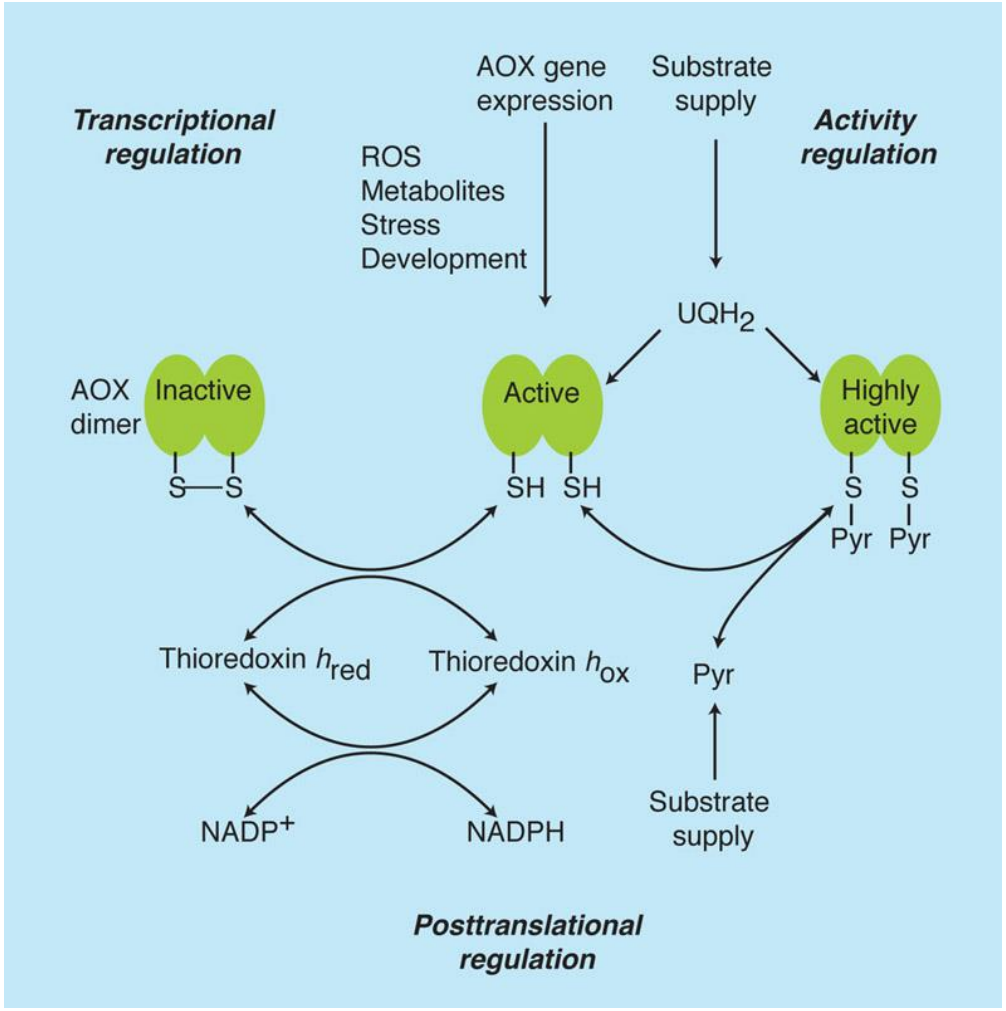

Post-translational regulation:

-AOX is embedded in the **inner leaflet of the inner mitochondrial membrane**, with the active site exposed to the **matrix**.

-The functional form of the enzyme is a **reduced dimer, non-covalently linked**.
The **two subunits of the AOX dimer** can be **covalently linked** through a **disulfide bridge (ponte disulfeto)** between **cysteine residues** (relatively inactive), a **thioredoxin system** converts this form into a **more active** form with free thiol groups **(reduced)**.

-Binding of pyruvate (Pyr) to the **reduced enzyme** and increases in the concentration of the substrate **ubiquinol** (UQH_2) inside the inner membrane and **increases activity.**

Thioredoxins regulate enzymes by **reducing disulfide bridges**. The presence of thioredoxin regulation connects the AOX activation level to the mitochondrial NADPH pool and the oxidation of citric acid cycle metabolites by NADP-utilizing enzymes.

AOX is generally present and expressed **in plants** and plant organs. It also occurs in some species of **fungi** and **protists**, and has even been found, contrary to previous beliefs, in several groups of **"primitive animals"** but not in vertebrates or arthropods (McDonald et al. 2009 doi:10.1242/jeb.032151).

Alternative Oxidase Isoforms Are Differentially Activated by Tricarboxylic Acid Cycle Intermediates[1][OPEN]

Plant Physiology®, February 2018, Vol. 176, pp. 1423–1432,

Arabidopsis thaliana has **five AOX isoforms** (AOX1A–AOX1D and AOX2). **AOX1D expression is increased in aox1a knockout mutants** from Arabidopsis but **cannot compensate for the lack of AOX1A**, suggesting a **difference in the regulation of these isoforms.**

Therefore, we analyzed the different AOX isoenzymes with the aim to identify differences in their posttranslational regulation. **Seven tricarboxylic acid cycle intermediates** (citrate, isocitrate, 2-oxoglutarate, succinate, fumarate, malate, and oxaloacetate) were tested for their influence on AOX1A, AOX1C, and AOX1D wild-type protein activity using a **refined in vitro system**.

Isolated mitochondria

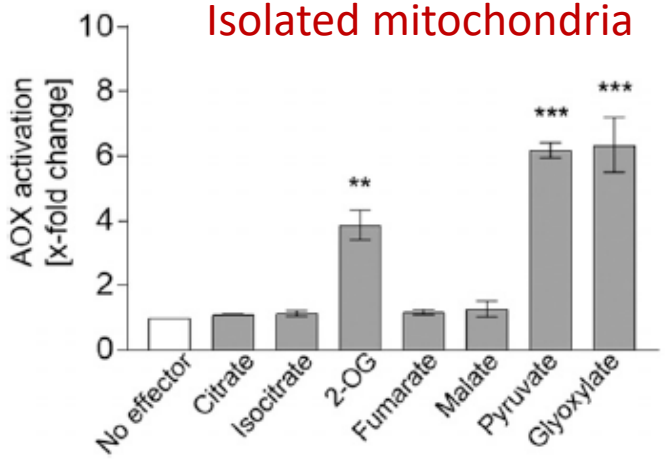

Figure 2. Influence of organic acids on the activity of the AOX pathway in plant mitochondria. The effect of different organic acids on the activity of the AOX pathway in isolated mitochondria from Arabidopsis was analyzed. AOX activity was determined as described by Jacoby et al. (2015) using 5 mM citrate, isocitrate, 2-OG, fumarate, malate, pyruvate, or glyoxylate as effectors. Measurements were carried out as three independent biological replicates. Each biological replicate was measured twice, leading to a total of six values per column. The basal activity (no effector) of the AOX pathway was 3.96 ± 0.6 nmol oxygen min^{-1} mg^{-1} protein. Asterisks indicate that the differences (**, $P < 0.01$ and ***, $P < 0.001$) between the basal activity (no effector) and activities in the presence of the effectors are statistically significant as determined by two-way ANOVA with posthoc Tukey's HSD test.

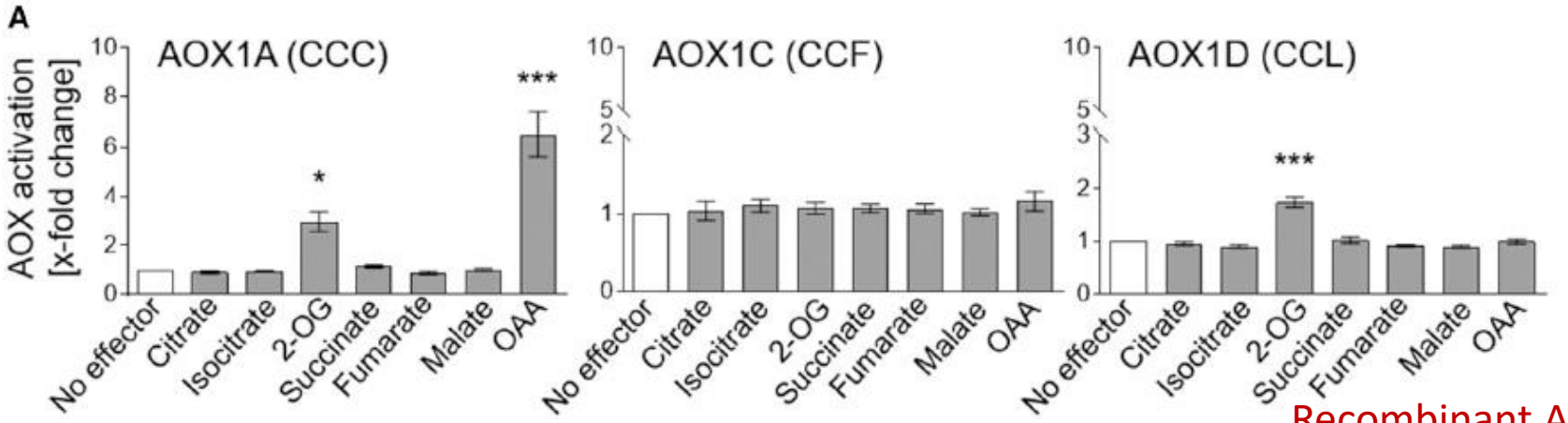

Figure 1. Influence of organic acids on the activity of AOX wild-type proteins. A, The effect of different organic acids on the activity of AOX1A-, AOX1C-, and AOX1D-WT proteins was analyzed. AOX activity was determined as described by Selinski et al. (2016) using 5 mM citrate, isocitrate, 2-OG, succinate, fumarate, malate, or OAA as effectors. Measurements were carried out as three independent biological replicates. Each biological replicate was measured twice, leading to a total of six values per column. Basal activities (no effector) were 5.7 ± 0.21 nmol oxygen min^{-1} density units $(DU)^{-1}$ for AOX1A-WT, 39.28 ± 3.94 nmol oxygen min^{-1} DU^{-1} for AOX1C-WT, and 15.26 ± 0.67 nmol oxygen min^{-1} DU^{-1} for AOX1D-WT. Asterisks indicate that the differences (*, $P < 0.05$ and ***, $P < 0.001$) between the basal activity (no effector) and activities in the presence of the effectors are statistically significant as determined by two-way ANOVA with posthoc Tukey's honestly significant difference (HSD) test. B, Schematic overview of AOX activation by TCAC intermediates.

Recombinant AOX proteins

each isoform was recombinantly expressed *in E. coli* BHH8, and membrane vesicles enriched in individual AOX proteins were isolated

Alternative Oxidase Isoforms Are Differentially Activated by Tricarboxylic Acid Cycle Intermediates[1][OPEN]

Plant Physiology®, February 2018, Vol. 176, pp. 1423–1432,

AOX1C is insensitive to all seven organic acids
AOX1A and AOX1D are both activated by 2-oxoglutarate
but **only AOX1A is additionally activated by oxaloacetate**.
Furthermore, **AOX isoforms cannot be transformed to mimic one another** by substituting the variable **cysteine residues** at position III in the protein.

AOX isoforms from Arabidopsis are **differentially fine-regulated by tricarboxylic acid cycle metabolites** (depending on the amino-terminal region around the highly conserved cysteine residues known to be involved in regulation by the 2-oxo acids pyruvate and glyoxylate) and propose that this is **the main reason why they cannot functionally compensate for each other.**

UCP in mammals

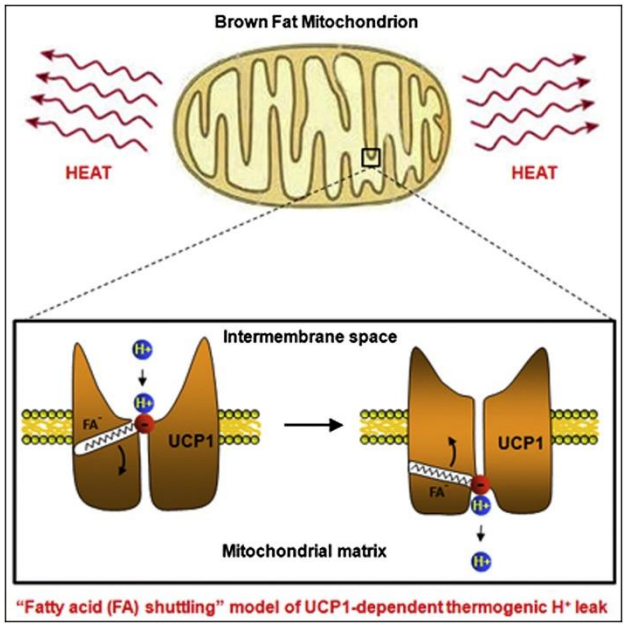

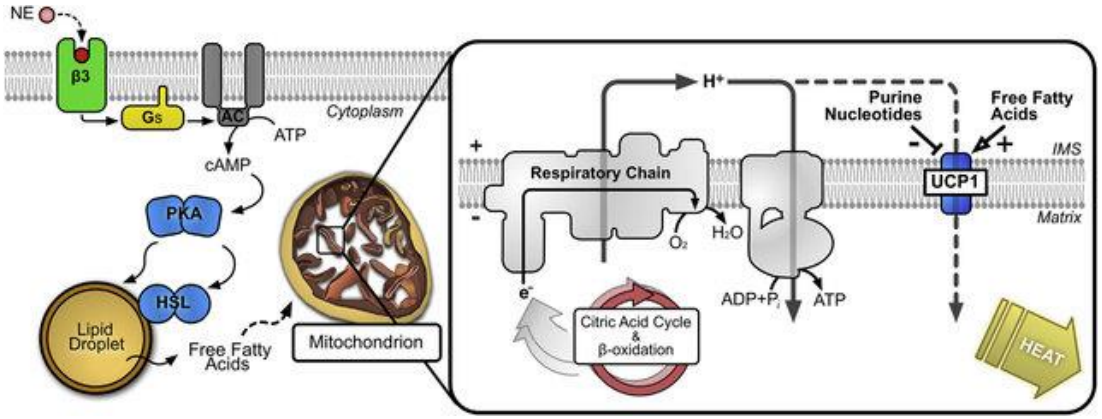

Upon **activation by long-chain fatty acids** (LCFAs), UCP1 increases the conductance of the inner mitochondrial membrane (IMM) to make Brown fat (BAT) mitochondria **generate heat rather than ATP.** Its activation by fatty acids, which overcomes its **inhibition by purine nucleotides (ATP, GTP)**

UCP1 has the same structural fold as **other mitochondrial carriers.** Is a **monomer,** binding **one purine nucleotide** and **three cardiolipin molecules tightly.**

GTP, produced in the Krebs cycle (conversion of succinyl Co-A into succinate) **under intense mitochondrial activity**, GTP concentration increases in the matrix to support RNA and protein synthesis together with the **inhibition of UCP** energy dissipation, thereby **promoting ATP synthesis**.

UCP in plants

FIG. 7. **Scheme of the interactions between mitochondrial membrane potential, ROS, and HNE production, UCP activity, and tricarboxylic acid cycle flux.** High mitochondrial membrane potential ($\Delta\psi$) leads to increased ROS production (*A*). Hydroxyl radicals initiate peroxidation of inner membrane lipids leading to production of HNE and other reactive alkenals (*B*). HNE activates UCP, which translocates protons from the intermembrane space into the matrix leading to a reduction in $\Delta\psi$ (*C*). Reduced $\Delta\psi$ facilitates higher tricarboxylic acid cycle flux (*D*) and reduces ROS production (*E*). Thus ROS act as a signal that activates a mechanism involving UCP to reduce ROS production. The activation of UCP by HNE and the consequences for $\Delta\psi$, tricarboxylic acid cycle flux, and ROS production are demonstrated in this study. The pathway leading from superoxide to HNE is inferred from our previous work, which demonstrates activation of potato UCP by superoxide (7) and by studies of the effect of a spin trap that reacts with carbon-centered radicals on proton conductance in animal mitochondria (10).

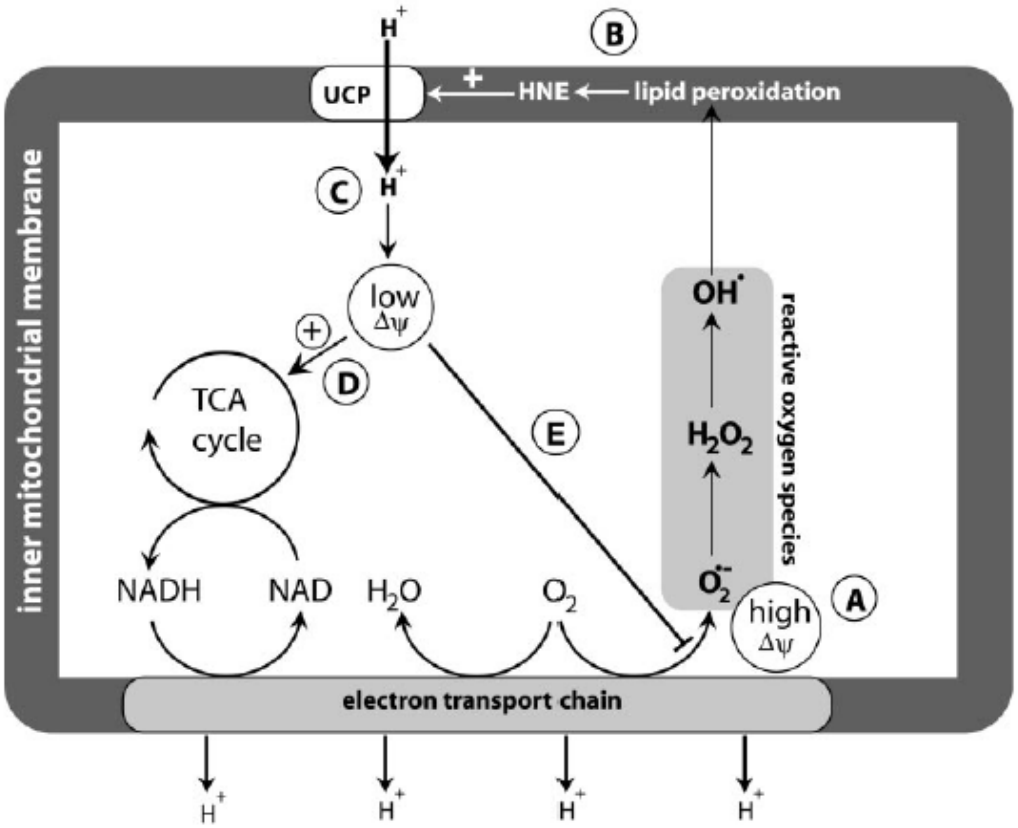

4-hydroxy-2-nonenal (HNE), a product of lipid peroxidation (and a structurally related compound, trans-retinal) stimulate a proton conductance in potato mitochondria that is inhibited by **GTP** (a characteristic inhibitor of UCP). It is questionable whether most plant organs present the FAs concentrations at the levels necessary to sustain UCP activity. Mitochondria isolated from plants are able to uncouple respiration even in the absence of added FFAs: It is possible that **phospholipases could provide FFAs** to support UCP activity.

PNAS | December 19, 2006 | vol. 103 | no. 51 | 19587–19592

Mitochondrial uncoupling protein is required for efficient photosynthesis

Lee J. Sweetlove*†, Anna Lytovchenko†, Megan Morgan*, Adriano Nunes-Nesi†, Nicolas L. Taylor*, Charles J. Baxter*, Ira Eickmeier†, and Alisdair R. Fernie†

*Department of Plant Sciences, University of Oxford, South Parks Road, Oxford OX1 3RB, United Kingdom; and †Max-Planck-Institute for Molecular Plant Physiology, Am Mühlenberg 1, 14476 Golm, Germany

a

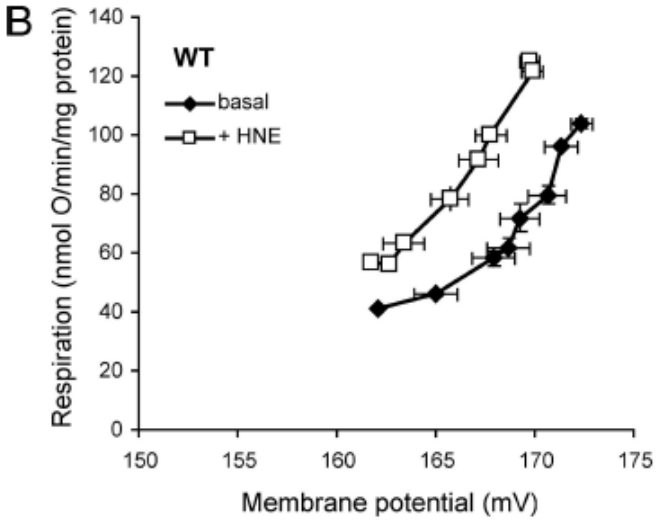

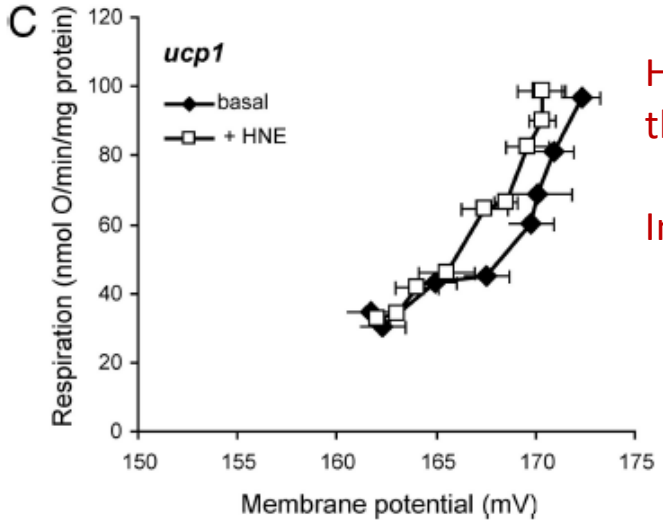

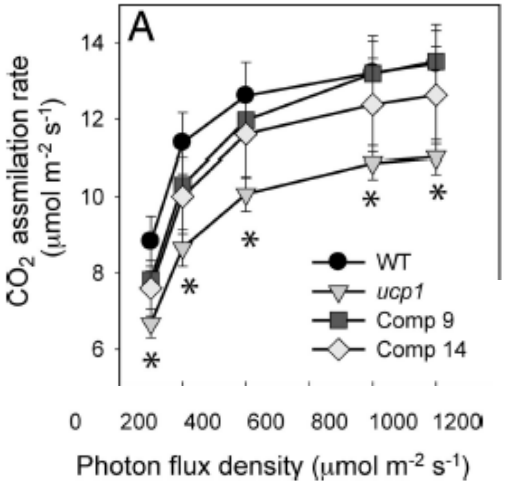

HNE: lipid peroxidation product that activates UCP

In Arabidopsis : UCP1, 2 and 4

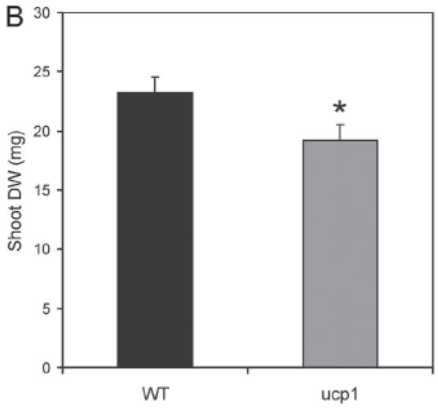

specific inhibition of photorespiration

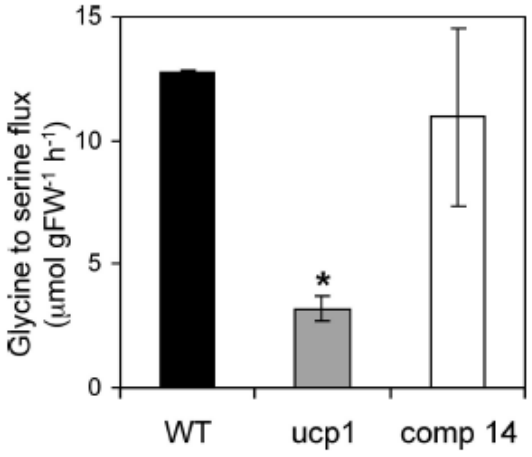

(*B*) UCP-catalyzed proton leak rate in mitochondria from WT is shown. (*C*) UCP-catalyzed proton leak rate in mitochondria from the *ucp1* mutant is shown. The basal proton leak rate (respiration in the absence of ATP synthase acitivity) and the UCP-catalyzed proton leak rate (respiration in the absence of ATP synthase activity and in the presence of HNE) are shown. Values are the means of three independent mitochondrial isolations ± SEM